Flight-Test Investigation of Certification Requirements for Laminar-Flow General Aviation Airplanes

G. S. Manuel*
NASA Langley Research Center, Hampton, Virginia 23665
and
W. A. Doty†
Cessna Aircraft Company, Wichita, Kansas 67277

A flight investigation has been conducted using a modified Cessna T210R to evaluate the performance, stability, and control characteristics of a general aviation airplane with significant natural laminar flow (NLF). Development of NLF technology for application to general-aviation-type aircraft requires an examination of the adequacy of existing certification requirements. The study focused on the aircraft's ability to meet certification requirements with significant NLF and also with the boundary-layer transition fixed near the leading edge. The investigation showed that large regions of NLF on the airplane's surfaces significantly enhanced cruise performance. Loss of laminar flow did not produce significant changes in the stability and control characteristics of this conventional configuration because of the well-designed NLF sections used. The research airplane met the Federal Aviation Regulations Part 23 certification requirements even though it was not intended to be certified.

Nomenclature

bhp = engine brake horsepower, ft-lb/s
F = force
kcas = calibrated airspeed, kt
L = left
R = right
STD = standard day condition
V = speed, ft/s
V_{S1} = stalling speed if obtainable, or minimum speed at which the airplane is controllable with the engine idling and propeller in takeoff position, kt
W = gross weight, lb
β = angle of sideslip, deg
ϕ = angle of bank, positive for right wing down, deg
δ_a = aileron deflection, positive trailing-edge down, deg
δ_e = elevator deflection, positive trailing-edge down, deg
δ_{et} = elevator tab deflection, positive trailing-edge down, deg
δ_r = rudder deflection, positive trailing-edge left, deg

Introduction

FOR the past decade, the NASA Langley Research Center has contributed to the development of natural laminar flow (NLF) technology for application to business, commuter, and transport aircraft.[1-4] The technology has been achievable in part through advanced NLF airfoil design and modern construction techniques using composites and milled or bonded aluminum skins. Airfoil design has emphasized development of airfoils with extensive NLF to reduce cruise drag without incurring a reduction in maximum lift or a change in pitching moment with the loss of NLF.

Application of NLF technology to new airplane designs has raised questions as to the adequacy of the existing Federal Aviation Regulations (FAR) Part 23 for certification of light airplanes having extensive laminar flow. In particular, both the Federal Aviation Administration (FAA) and the general aviation industry are concerned whether the existing criteria adequately address any stability and control problems that could occur in the event of partial or total loss of laminar flow.

During 1989, flight experiments were conducted under a joint NASA, Cessna Aircraft, and FAA program to address the applicability of existing procedures and standards for certification of airplanes with extensive regions of NLF. These

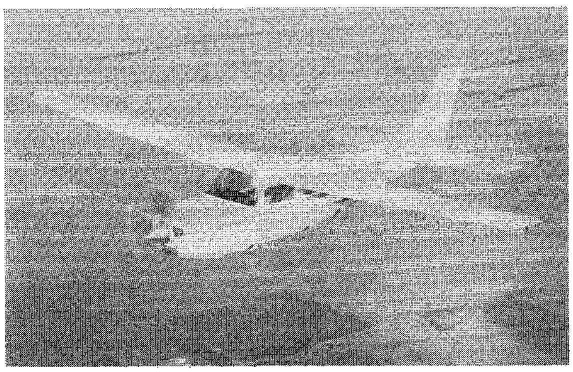

Fig. 1 Modified research airplane.

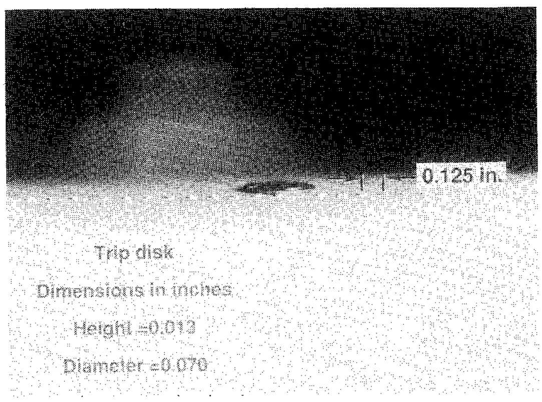

Fig. 2 Photograph of the artificial boundary-layer transition method using trip disks.

Received March 22, 1990; presented as Paper 90-1310 at the AIAA 5th Flight Test Conference, Ontario, CA, May 21–24, 1990; revision received Sept. 17, 1990; accepted for publication Oct. 3, 1990. Copyright © 1990 by the American Institute of Aeronautics and Astronautics, Inc. No copyright is asserted in the United States under Title 17, U.S. Code. The U.S. Government has a royalty-free license to exercise all rights under the copyright claimed herein for Governmental purposes. All other rights are reserved by the copyright owner.
*Research Engineer, Mail Stop 247.
†Engineer. Member AIAA.

tests utilized a modified Cessna T210R airplane having a wing with a NASA-designed NLF(1)-0414F airfoil section, an NLF horizontal stabilizer, and a smoothed vertical stabilizer (Fig. 1). Flight tests simulated FAR Part 23 certification tests, which evaluate performance and stability and control characteristics. Tests and parameters, which could be affected by the loss of laminar flow, were chosen to allow quantitative comparison of the airplane's ability to meet certification requirements. Several combinations of laminar and turbulent boundary-layer configurations on the airplane's wing and tail surfaces were explored. Results are presented for the following airplane boundary-layer configurations: 1) natural transition on all surfaces, 2) fixed transition at 5% chord on upper and lower surfaces of the wing and horizontal stabilizer and both sides of the vertical stabilizer, and 3) fixed transition at 5% chord on the upper and lower surfaces of the left wing and the remaining surfaces with natural transition.

Airplane Description

The single-engine conventional configuration was evaluated in the study. A photograph of the research airplane is presented in Fig. 1. The airplane's production engine was replaced with a TSI0-520-CE rated at 325 bhp at 2700 rpm, which allowed for the installation of dual alternators to provide for the additional electrical needs of the instrumentation package.

The airplane was modified for research by incorporating an NLF wing and horizontal stabilizer, and a smoothed vertical stabilizer. The modified wing had zero twist, a span of 42 ft and an aspect ratio of 11. The wing incorporated a natural laminar flow NLF(1)-0414F airfoil section[3-5] and incorporated a 12.5% chord trailing-edge cruise flap that was fixed in the cruise position during this investigation. To obtain the desired airfoil section contours, a polyester resin filler material was used over an aluminum wing skin. The NLF airfoil section was designed to achieve low drag at a cruise Reynolds number of 10×10^6 by maintaining NLF to about 70% chord on both the upper and lower surfaces. Earlier full-scale wind-tunnel and flight tests of this airplane were reported in Refs. 6 and 7, respectively.

The horizontal and vertical stabilizers were modified from the production configuration. The production horizontal stabilizer used NACA 0012 and NACA 0010 airfoil sections at the root and tip, respectively. The design goal of this modification was to create a laminar flow section with a wide drag bucket and provide a large range of useful lift coefficients. The horizontal stabilizer was recontoured to a cambered airfoil section by adding a 12.5% chord extension forward of the production leading edge. Foam filler was wrapped around the leading edge and was contoured using a polyester resin filler material. This method allowed the production elevator to be retained. The production vertical stabilizer and dorsal fin production airfoil sections were smoothed by recessing rivets below the surface and filling imperfections from the leading edge to the 50% chord location. The waviness of the horizontal and vertical stabilizer surfaces when measured in a chordwise direction was maintained within ± 0.003 in. per 2 in. of wavelength.

Since the horizontal and vertical stabilizer modifications created additional weight in the empennage area, all research flights were conducted beyond the production aft c.g. limit. Airframe modifications, instrumentation, and ballast resulted in a test gross weight of 4100 lb, which is greater than that of the production T210R.

Onboard instrumentation recorded airspeed and flow angles ahead of each wing tip, altitude, control forces, control surface positions, engine speed and power output, and linear accelerations and angular rates along and about the body axes, respectively. Wing and horizontal-stabilizer surface pressures and hot-film sensor outputs were recorded to assist in verification of the extent of NLF on these surfaces.

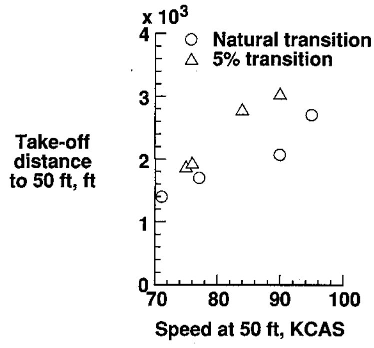

Fig. 3 Effect of transition location on takeoff performance.

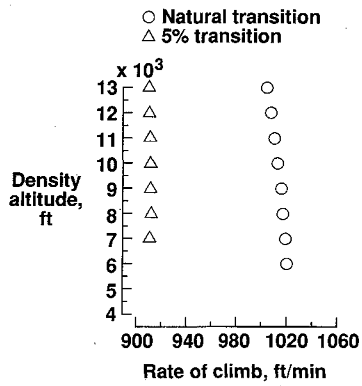

Fig. 4 Effect of transition location on rate of climb at 100 kcas.

Test Matrix and Data Standardization

The flight-test maneuvers performed followed a typical FAA certification flight-test matrix. The matrix addressed performance, stability, controllability, and trim characteristics as required by the FAA, and was repeated for each of the airplane transition configurations.[8]

Engine power was corrected to standard day and sea level conditions, using methods outlined in Ref. 9. Airspeed was corrected to standard weight for takeoff and climbs by the following relationship:

$$V_{STD} = V_{TEST} \sqrt{W_{STD}/W_{TEST}}$$

The propeller slipstream has a rotational component that changes the angle of attack of the vertical tail and creates sideslip if uncorrected by the rudder. Slipstream rotation is most significant for high power at low speed. To account for this effect in the directional trim tests, rudder deflection required for steady heading was plotted against power divided by airspeed.[10]

Flight-Test Results

Transition Location

The extent of NLF on all modified surfaces was verified using two different techniques. The sublimating-chemical-boundary-layer-flow visualization technique and hot-film sensors were used to determine the chordwise location at which the laminar boundary layer transitioned to a turbulent boundary layer on the wing and the horizontal stabilizer.

Laminar flow was maintained on both the upper and lower surfaces of the wing from the leading edge aft to about 70% chord at and above 100 kcas. On the horizontal stabilizer, laminar flow was achieved from the leading edge aft to 70% chord on the upper surface at and above 100 kcas, 50% chord on the lower surface at 100 kcas, and about 35% chord on the lower surface at 150 kcas. On the vertical stabilizer, laminar flow was maintained from the leading edge aft to 50% chord on the lower half of the stabilizer at and above 100 kcas and

Table 1 Transition effects on airspeed

	Airspeed, kcas	
Configuration	75% MCP	100% MCP
Natural transition	155	178
Asymmetric transition	152	167
5% transition	150	162

30% chord on the upper half of the stabilizer at and above 100 kcas.

The sublimating chemical technique was also used to determine the effectiveness of a new method of fixing transition using trip disks. For this technique, tape with evenly spaced circular holes was secured spanwise along the 5% chord location. The holes were filled with polyester resin filler material and were allowed to dry. When the tape was removed, the trip disks remained secured to the leading-edge surface. The trip disks measured 0.013 in. high, 0.070 in. diam, and were spaced 0.125 in. center to center, as shown in Fig. 2. All fixed transition tests were conducted with the trip disks located at 5% chord of the upper and lower surfaces of the wing, horizontal tail, and both sides of the vertical tin. Flow visualization research flights to verify transition location showed the trip disks were effective at fixing transition at the 5% chord location.

Performance

Takeoff

Takeoff distance, as outlined in FAR 23.51, is the distance required to take off and clear a 50-ft obstacle. Takeoff tests were performed with takeoff power and with flaps retracted. Average winds at 6 ft above ground level were below 10 kt for all tests. Takeoff distance was recorded from standing start to 50-ft altitude using radar and a microwave distance measuring unit system. The approximate climb airspeed was 1.3 V_{S1}, which equaled 87.2 kcas. All data were corrected to a standard weight of 4100 lb, power was corrected to standard day, and distance through the air was corrected to zero wind. Takeoff and rate-of-climb data are presented for the 5% and natural transition configurations only.

Takeoff performance data are presented in Fig. 3. At 87.2 kcas, takeoff distance increased from approximately 2160 ft with natural transition to approximately 2760 ft with transition fixed at 5% chord. Most of the increase occurred in the distance through the air. This increase was greater than expected, even considering that the airplane was accelerating.

Climb

Similar to the takeoff performance data, climb rates and gradients for the two different airplane transition configurations were acceptable under FAR Part 23. Requirements for minimum climb rates and gradients are presented in FAR 23.65. When comparing boundary-layer transition location effects, changes in climb rates and gradients are of more interest than individual magnitudes. Thus, continuous climbs were performed from 7000 to 13,000 ft density altitude at 100 kcas with maximum continuous power. To correct for wind effects, each climb was repeated with the opposite heading and always perpendicular to the reported winds. Tests were performed in smooth air with standard lapse rates to avoid rising or sinking air masses. Climb data were corrected for a standard weight of 4100 lb, and power was corrected for standard temperatures. Climb rate was determined from the slope of the plots of corrected density altitude vs time. Results for each pair of opposite headings were averaged to obtain final climb rates.

Rate-of-climb data corrected for standard day conditions are presented in Fig. 4. At 10,000 ft density altitude, rate of climb decreased from 1013 ft/min for natural transition to 912 ft/min for transition at 5% chord. This represented a 10% rate of climb degradation.

Cruise

Although cruise speed is not addressed by FAR Part 23, large cruise performance changes were realized with the loss of NLF as seen in Table 1. At 100% maximum continuous power (MCP), natural laminar flow from the leading edge aft to 70% chord improved cruise speed approximately 10% compared to the configuration with transition at 5% chord.

Stability and Control

Unlike the performance data that showed a degradation with the loss of NLF, all static lateral-directional and longitudinal stability and control maneuvers showed negligible differences among the three different transition configurations. FAR 23.177 outlines the stability and control requirements. Flight maneuvers were designed to determine the airplane's ability to meet the specified certification requirements with boundary-layer changes.

For stability tests, the pilot maintained steady heading sideslips at several aileron deflections from full left to full right at two different power/speed conditions: idle power at 100 kcas to minimize power effects on the data, and cruise at 75% MCP. For the idle power condition, altitude varied; for the cruise condition, airspeed varied among the configurations due to changes in drag.

Lateral/Directional

Figure 5 presents a quantitative comparison among the transition configurations for the lateral/directional stability flight maneuvers by comparing control deflections and bank angle with sideslip angle. The control surface deflections required for steady heading sideslip at idle power did not change significantly among transition configurations. There was no appre-

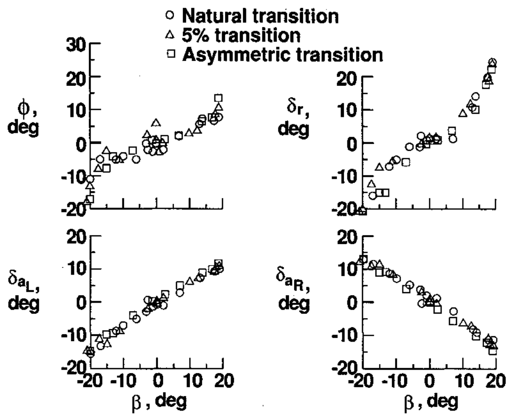

Fig. 5 Effect of transition location on static lateral-directional stability at 100 kcas and idle power.

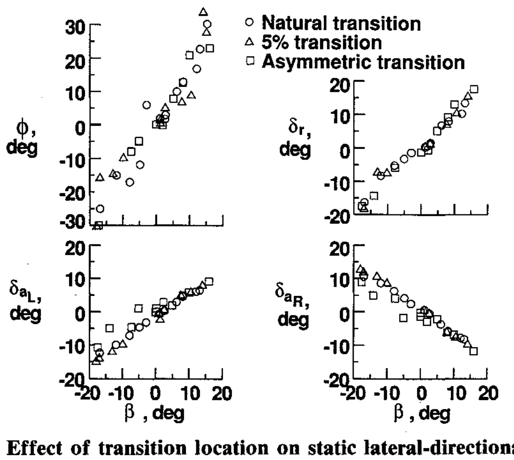

Fig. 6 Effect of transition location on static lateral-directional stability at 75% MCP.

ciable difference in the relationship between bank and sideslip angle.

Figure 6 shows that the control surface deflections required for steady heading sideslip at MCP did not change significantly between the natural and 5% transition configurations. For the asymmetric transition configuration at negative sideslip angles, less aileron input is required to hold a steady heading. This result may have been caused by the additional drag of the tripped left wing.

Like the stability results, the airplane control characteristics remained within FAR 23.177, paragraph 3 certification requirements with negligible change among the transition configurations. As seen in Fig. 7, the aileron and rudder control forces required for steady heading sideslip with idle power for all three configurations were indistinguishable. As required, the aileron and rudder forces increased steadily with increased sideslip angle.

Figure 8 shows that for the MCP condition, more aileron force was required with the asymmetric configuration for steady heading sideslip in comparison to the other configurations. The required aileron force difference is less than 10 lb. Also, the rudder force for the asymmetric transition configuration showed a trend toward less force for positive sideslip angles and more force for negative angles. This is attributed to the asymmetric drag of the wing.

Trim

Longitudinal trim requirements are specified in FAR 23.161 (c). For a quantitative comparison, elevator trim tab deflection required to trim the airplane longitudinally from the minimum trimmable airspeed to the maximum allowable flight speed was measured for the different configurations. Figure 9 shows there were no major differences between the elevator trim tab deflections required for the different configurations. However, there was a slight increase in elevator trim tab deflection with 5% transition over that required for the other

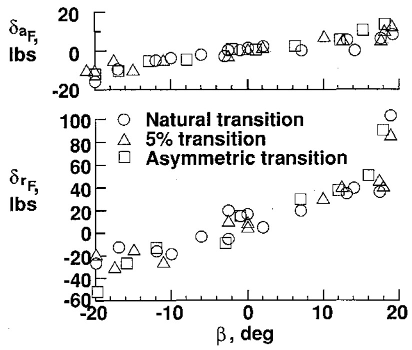

Fig. 7 Effect of transition location on static lateral-directional control at 100 kcas and idle power.

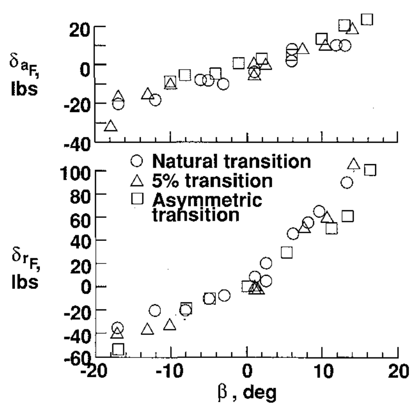

Fig. 8 Effect of transition location on static lateral-directional control at 75% MCP.

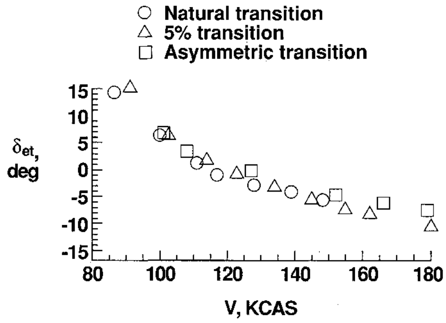

Fig. 9 Effect of transition location on elevator trim tab required for level flight.

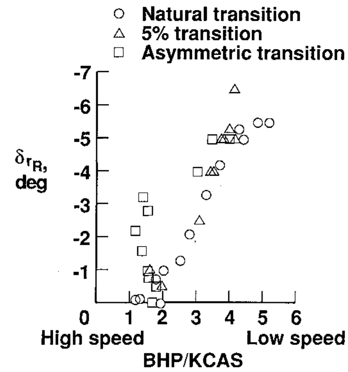

Fig. 10 Effect of transition location on rudder trim required for level flight.

transition configurations. This deflection increase of about 4 deg may have been due to a thicker boundary layer at the trailing edge of the horizontal stabilizer with the 5% transition configuration.

Directional trim requirements, which are specified in FAR 23.161(b), state that the airplane must be trimmable in level flight. Flight maneuvers compared the potential changes in the airplane's ability to meet this requirement with changes in the boundary layer by investigating the rudder deflection required to directionally trim the aircraft. Rudder deflection required to trim the airplane was measured during steady heading flight over a range of speeds and was plotted against engine brake horsepower divided by calibrated airspeed for the tests.

The natural and 5% transition airplane configurations showed no appreciable difference in rudder required for trim, as seen in Fig. 10. In contrast, the asymmetric configuration showed more rudder was required at high speed in comparison to the other configurations. The amount of rudder required at high speed was still less than that required in all configurations for low-speed and high-power conditions. Thus, a rudder sized for takeoff conditions would suffice for all other flight regimes.

Summary of Results

A flight investigation has been conducted using a modified Cessna T210R to evaluate the performance, stability, and control characteristics of a general aviation airplane with significant natural laminar flow (NLF). Development of NLF technology for application to general aviation type aircraft has resulted in an examination of the adequacy of the existing certification requirements. The study focused on potential changes in the aircraft's ability to meet certification requirements with significant NLF and with the boundary-layer transition fixed near the leading edge. The most significant results of this study to evaluate the research airplane's aerodynamic changes with the loss of NLF and its compliance with FAR Part 23 can be summarized as follows:

1) The loss of natural laminar flow, both symmetrically and asymmetrically, did not produce significant lateral-directional

stability and control changes. The airplane exhibited no stability and control behavior that was unacceptable under FAR Part 23 requirements.

2) Climb performance decreased 10% when the boundary layer was tripped and laminar flow was restricted to the first 5% of the laminar flow surfaces. These losses were consistent with the expected drag increase associated with the tripped boundary layer.

References

[1]Holmes, B. J., Obara, C. J., and Yip, L. P., "Natural Laminar Flow Experiments on Modern Airplane Surfaces," NASA TP-2256, June 1984.

[2]Somers, D. M., "Design and Experimental Results for a Natural-Laminar Flow Airfoil for General Aviation Application," NASA TP-1861, 1981.

[3]Viken, J. K., "Aerodynamic Design Considerations and Theoretical Results for a High Reynolds Number Natural Laminar Flow Airfoil," M.S. Thesis, George Washington Univ., Washington, DC, Jan. 1983.

[4]McGhee, R. J., Viken, J. K., Pfenninger, W., Beasley, W. D., and Harvey, W. D., "Experimental Results for a Flapped Natural-Laminar-Flow Airfoil with High Lift/Drag Ratio," NASA TM-85788, May 1984.

[5]Viken, J. K., Campbell, R. L., Viken, S. A. W., Pfenninger, W., and Morgan, H. L., Jr., "Design of the Low-Speed NLF-0414 and the High-Speed NLF-0213 Airfoils with High-Lift Systems," Natural Laminar Flow and Laminar Flow Control Symposium, NASA Langley Research Center, Hampton, VA, March 16–19, 1987.

[6]Murri, D. G., and Jordon, F. L., Jr., "Wind-Tunnel Investigation of a Full-Scale General Aviation Airplane Equipped with an Advanced Natural Laminar Flow Wing," NASA TP-2772, Nov. 1987.

[7]Befus, J., Nelson, R., Latas, J., Sr., and Ellis, D., "Flight Test Investigations of a Wing Designed for Natural Laminar Flow," General Aviation Aircraft Meeting and Exposition, SAE-871044, Society of Automotive Engineers, April 1987.

[8]"Airworthiness Standards; Normal, Utility, Acrobatic, and Commuter Category Airplanes," *Code of Federal Regulations, Title 14, Aeronautics and Space*, Pt. 23, Office of the Federal Register National Archives and Records Administration, Jan. 1988, pp. 103–246.

[9]Teledyne Continental Motors TSIO-520-CE Model, Aircraft Products Div., Mobile, AL, Jan. 1984.

[10]Perkins, C. D., and Hage, R. E., *Airplane Performance Stability and Control*, Wiley, New York, 1967.

Recommended Reading from the AIAA Progress in Astronautics and Aeronautics Series . . . AIAA

Dynamics of Flames and Reactive Systems and Dynamics of Shock Waves, Explosions, and Detonations

J. R. Bowen, N. Manson, A. K. Oppenheim, and R. I. Soloukhin, editors

The dynamics of explosions is concerned principally with the interrelationship between the rate processes of energy deposition in a compressible medium and its concurrent nonsteady flow as it occurs typically in explosion phenomena. Dynamics of reactive systems is a broader term referring to the processes of coupling between the dynamics of fluid flow and molecular transformations in reactive media occurring in any combustion system. *Dynamics of Flames and Reactive Systems* covers premixed flames, diffusion flames, turbulent combustion, constant volume combustion, spray combustion nonequilibrium flows, and combustion diagnostics. *Dynamics of Shock Waves, Explosions and Detonations* covers detonations in gaseous mixtures, detonations in two-phase systems, condensed explosives, explosions and interactions.

Dynamics of Flames and Reactive Systems
1985 766 pp. illus., Hardback
ISBN 0-915928-92-2
AIAA Members $59.95
Nonmembers $92.95
Order Number V-95

Dynamics of Shock Waves, Explosions and Detonations
1985 595 pp., illus. Hardback
ISBN 0-915928-91-4
AIAA Members $54.95
Nonmembers $86.95
Order Number V-94

***TO ORDER:* Write, Phone or FAX:** American Institute of Aeronautics and Astronautics, c/o TASCO, 9 Jay Gould Ct., P.O. Box 753, Waldorf, MD 20604 Phone (301) 645-5643, Dept. 415 FAX (301) 843-0159

Sales Tax: CA residents, 7%; DC, 6%. Add $4.75 for shipping and handling of 1 to 4 books (Call for rates on higher quantities). Orders under $50.00 must be prepaid. Foreign orders must be prepaid. Please allow 4 weeks for delivery. Prices are subject to change without notice. Returns will be accepted within 15 days.